Mechanism for CO Oxidation and Oscillatory Reactions on Pd Tip and Pd(110) Surfaces: FEM, TPR, XPS Studies

V. V. GORODETSKII[1], A. V. MATVEEV[1], A. V. KALINKIN[1] and B. E. NIEUWENHUYS[2]

[1]*G. K. Boreskov Institute of Catalysis, Siberian Branch of the Russian Academy of Sciences, Pr. Akademika Lavrentyeva 5, Novosibirsk 630090 (Russia)*
E-mail: gorodetsk@catalysis.nsk.su
[2]*Leiden Institute of Chemistry, P. O. Box 9502, 2300 RA Leiden (The Netherlands)*

Abstract

Detailed studies of the coadsorption of oxygen and carbon monoxide, hysteresis phenomena and oscillatory reaction of CO oxidation on Pd(110) and Pd tip surfaces have been carried out with the molecular beam (MB), field electron microscope (FEM), temperature programmed reaction (TPR) and X-ray photoelectron spectroscopy (XPS). It has been found that the occurrence of kinetic oscillations over Pd surfaces is associated with periodic formation and depletion of subsurface oxygen (O_{sub}). Transient kinetic experiments show that CO does not react chemically with subsurface oxygen to form CO_2 below 300 K. It has been found that CO does react with an atomic O_{ads}/O_{sub} state beginning at temperature ~150 K. Analysis of Pd tip surface with a local resolution of ~20 Å shows the availability of a sharp boundary between the mobile CO_{ads} and O_{ads} fronts.

INTRODUCTION

Unslackened interest in self-oscillatory phenomena in catalytic reaction over metal surfaces [1] is for a large part caused by the possibility to perform the catalytic processes more effectively using the unsteady-state operation. The extensive study of model reactions (CO + O_2, CO + NO, NO_x reduction, *etc.*) has been stimulated by the relevance of these reactions to an air pollution control [2]. The automotive catalyst is based on the precious metals, usually Pt, Rh or Pd. The CO oxidation and NO_x reduction on noble metal surfaces are highly non-linear systems. Usually these reactions are operated under conditions far from the thermodynamic equilibrium, where temporal and spatial organization becomes possible. In the oscillating regime of the reactions, the reaction mixture periodically affects the metals properties. These processes can be accompanied by (i) surface phase transition; (ii) facetting of the surface; (iii) formation of oxide layers. Two different mesoscopic and microscopic analytical tools have been introduced and successfully applied to learn details about the reaction dynamics at catalyst surfaces [3]. During catalytic reactions the formation of the target pattern and the propagation of reaction-diffusion fronts were observed [3–8]. Inspired by these experimental results Field Electron Microscopy (FEM) with higher lateral resolution of ~20 Å and Field Ion Microscopy with atomic resolution of ~3–6 Å have been developed to investigate a dynamic surface phenomena at CO oxidation over Pt tip surfaces. Sharp tips of Pt and Rh in size up to several hundreds of Angströms have been used to perform in situ investigations of real dynamic surface processes in which different crystallographic nanoplanes of the emitter-tip are simultaneously exposed to the reacting gas [4–7]. These tips were used for the first time as an excellent model for metal supported catalyst to study oscillations in CO + O_2, NO + H_2, H_2 + O_2 reactions *in situ*. The principal result of these studies was that non-linear reaction kinetics is not restricted to macroscopic planes since: (i) the planes ~200 Å in diameter show the same non-linear kinetics; (ii) regular waves appear under the reaction rate oscillations; (iii) the propagation of reaction-diffusion waves includes

the participation of the different crystal nanoplanes and indicates an effective coupling of adjacent planes.

It is well known that the Langmuir – Hinshelwood mechanism is used to describe the CO oxidation on platinum group metals. In order to explain the occurrence of kinetic oscillations an additional feedback reaction is required. Mechanisms of these oscillations on the platinum surfaces are connected with the surface reconstruction {Pt(100)-(hex) ↔ (1×1)} [8]. The palladium surfaces are known not to reconstruct and isothermal oscillations are associated with subsurface oxygen formation (Pd(110): $O_{ads} \Leftrightarrow O_{sub}$) [9].

The reaction kinetics on the Pd tip (model catalyst, grain diameter ~10^3 Å) might be quite various as compared to that on the single crystal surfaces as a result of an interplay between different nanoplanes present on emitter surfaces [4]. On the supported metal catalyst with a crystallite size of ~500 Å, these surfaces are formed by the most dense (111), (100), (110) nanoplanes which differ dramatically in adsorption and oscillation behaviour.

In the present work the mechanism of surface waves generation in the oscillating CO + O_2 reaction has been studied on a Pd tip (~2000 Å in radius) by a FEM that is responsible for experimental tool for *in situ* imaging of real dynamic surface processes in which different nanoplanes of emitter-tip are simultaneously exposed to the reacting gas. The O_2 adsorption and the reaction of atomic O_{ads} state as well as a subsurface atomic O_{sub} state with CO on the Pd(110) single crystal surface have been studied by TDS, TPR and XPS techniques. The hysteresis phenomena and oscillations of CO + O_2 reaction have been studied by means of molecular beam (MB) techniques. The effect of subsurface oxygen state on the subsequent CO_{ads} + O_{ads} reaction at an oxygen preadsorbed Pd(110) surface has been studied with TPR techniques.

EXPERIMENTAL

Experiments were performed in a UHV chamber (base pressure <10^{-10} mbar) which was used simultaneously as the catalytic reactor and field electron microscope. The catalyst was a Pd-emitter tip of a small radius (~2000 Å), prepared from spectroscopically pure Pd-wire (0.1 mm ∅), spot-welded to a metal heating loop of 0.25 mm diameter. The method for producing clean stable Pd tips, along with the experimental set-up has also been described elsewhere [10]. The temperature at the tip could be controlled to within 1 K and it was measured by means of a chromel/alumel thermocouple spot-welded to the metal loop near the tip. The reaction gases CO and O_2 of highest purity were introduced with a flow rate of 2.5 L s^{-1} and controlled by a quadrupole mass spectrometer. The total field electron current and FEM image were continuously monitored during the catalytic surface reaction at an oxygen partial pressure of ≈10^{-3} mbar and carbon monoxide partial pressure of ≈10^{-4} mbar. A double channel plate was used as an image amplifier of a small electron emission current (<1 nA), and CCD camera recorded the behaviour of the catalytic CO oxidation *in situ*. It was demonstrated that at a pressure of up to ≈10^{-3} mbar, stable emission currents could be obtained and sputtering processes omitted. The surface analysis of the Pd emitter is based on the fact that due to adsorption of CO and oxygen, local work function changes ($\Delta\Phi$) can be correlated with the total field electron current, as described before [10]. Electrostatic field effects at a field of ~0.4 V/Å during these investigations have not been obvious in according with [11].

The TDS and TPR experimental device on the single crystal Pd(110) surface is described in detail in [12]. The UHV chamber is equipped with a VG QXK 400 quadrupole mass spectrometer, a sputtering ion gun and molecular beam doser. A detailed description of doser setup is given in [13]. The TD spectra were obtained with a heating rate of 6 K s^{-1}. Steady-state rates and oscillations for the catalytic CO + O_2 reaction on Pd(110) surfaces have been measured by using a molecular beam setup with mass spectrometry detection. The crystal is exposed to CO + O_2 molecular beam through a capillary array doser with the gas flow controlled by mass spectrometer. XPS part of the present work was performed over Pd foil on

the basis of an X-ray photoelectron spectrometer VG ESCA-3.

RESULTS AND DISCUSSION

Carbon monoxide and oxygen adsorption

WF. At 300 K, the work function ($\Delta\Phi$) over Pd tip increases with an increase of oxygen exposure up to a value of 0.37 eV above that of the clean surface. This value compared to $\Delta\Phi$ = 0.4 eV for the Pd(110) single crystal surface at T_{ads} = 304 K [14]. This value is already reached at O_2 exposure of ~2.3 10^{-6} mbar (Fig. 1), suggesting a sticking probability near unity. The change in work function ($\Delta\Phi$ = 0.98 eV) with CO exposure on Pd tip at 300 K is shown in Fig. 1. Similar measurements at 300 K on Rh tips led to changes in work function, $\Delta\Phi$ = 1.20 eV [15]. Measurements on different Pd single crystal surfaces give a maximum increase in work function in the range 0.75–1.27 eV for the various planes, with Pd(111) showing a maximum increase of 0.98 eV [16]. The work function variation with coverage was used for determination of the isosteric heat of CO adsorption on the clean Pd tip surface. This value was found to be ~154 kJ mol^{-1} in the limit of zero coverage, decreasing to ~133 kJ mol^{-1} at coverage of 0.5 ML (monolayer) [10].

TDS. Figure 2 illustrates a series of CO TD spectra as a function of exposure. During CO adsorption at 100 K on the Pd(110) surface several molecular CO_{ads} states with the desorption peak temperatures at 230 (α_1), 280 (α_2), 330 (α_3) and 410 (β_1), 470 K (β_2) appear (see Fig. 2) to be in agreement with [17].

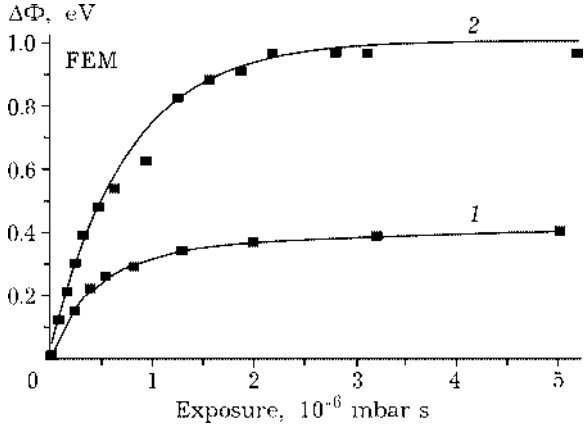

Fig. 1. Change in work function *versus* exposure of O_2 (*1*) and CO (*2*) on Pd at 300 K, using the simplified Fowler – Nordheim equation. $P(CO) = P(O_2) = 5\ 10^{-9}$ mbar.

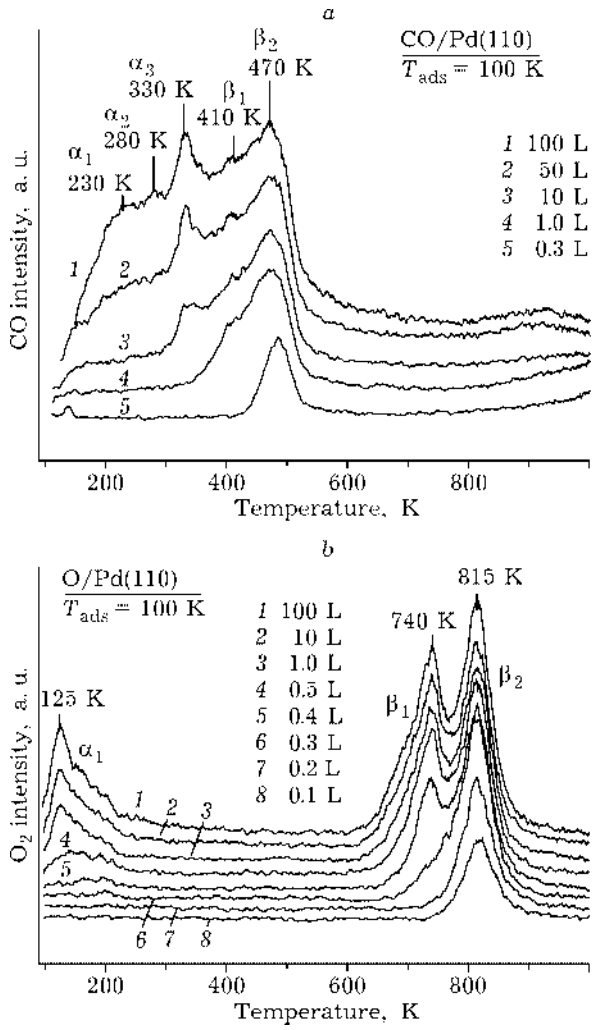

Fig. 2. Temperature desorption spectra of carbon monoxide (*a*) and of oxygen (*b*) from Pd(110) exposed at T_{ads} = 100 K.

Figure 2, *b* shows TD spectra of O_2 from Pd(110) surface after different oxygen exposures at 100 K. Above 0.3 L exposure (1 L = 1.33 10^{-6} mbar), there are three peaks in the TD spectrum located around 125 (α_1-O_2 molecular state) and 740 (β_1-O_{sub} subsurface atomic state) and 815 K (β_2-O_{ads} surface atomic state). The β_1-oxygen state was attributed to subsurface layer oxygen formation ($O_{ads} + *_v \rightarrow [*O_{sub}]$) as a result of appearance of efficient desorption channel for recombination of oxygen adatoms in the atomic states: $[*O_{sub}] + [*O_{sub}] \rightarrow O_2 + 2*_v$, where $*_v$ is a subsurface empty site. In the O/Pd(110) system, indirect evidence for the for-

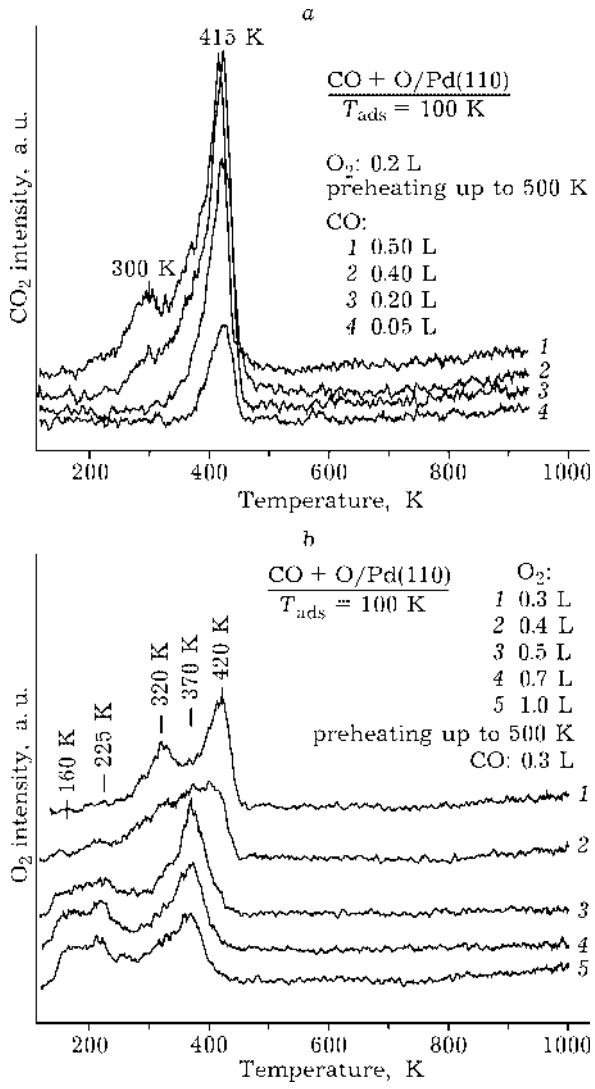

Fig. 3. Temperature programmed reaction of CO_2 formation from β_2-O_{ads} (*a*) and β_1-O_{sub} + β_2-O_{ads} atomic oxygen layers (*b*).

mation of subsurface oxygen layer during adsorption comes from the work function measurements [18].

TPR. The effect of subsurface oxygen layer formation on the CO + O_{ads} → CO_2 reaction rate has been studied by temperature programmed reaction experiments. Figure 3, *a* shows the TPR spectra of coadsorbed oxygen and carbon monoxide. Oxygen was adsorbed first to small coverage (θ ~ 0.2 ML) in atomic β_2-O_{ads} state, followed by CO exposure at 100 K. CO_2 is evolved mainly in a peak at 415 K and in a small peak at 300 K as a result of CO exposure.

Figure 3, *b* depicts the TPR spectra of coadsorbed oxygen (atomic β_2-O_{ads} and β_1-O_{sub} states)

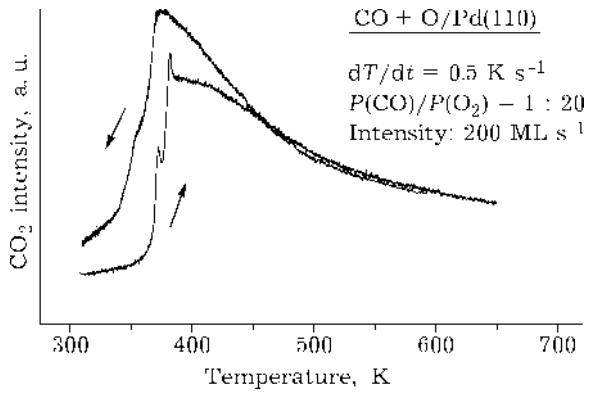

Fig. 4. The hysteresis of steady-state rates of CO_2 formation during a heating-cooling cycle at an CO + O_2 molecular beam pressure.

and CO. In contrast to Fig. 3, *a*, low temperature CO_2 formation begins immediately above oxygen exposure 0.5 L. Five distinct CO_2 desorption peaks are observed at 160, 225, 320, 370, and 420 K from the (110) surface. The complexity of CO_2 formation may be the result of different reaction rates of adsorbed CO with two types of adsorbed atomic oxygen: 1) $CO_{ads} + O_{ads} \rightarrow CO_{2\ gas} + 2*$; 2) $CO_{ads} + [*O_{sub}] \rightarrow CO_{2\ gas} + 2* + *_v$. In addition the reaction complexity might be expected since the coadsorption of CO and oxygen may result in the formation of either a segregated layer, where the CO_{ads} molecules and O_{ads} atoms form separate layer on the surface, or a mixed layer where the two adsorbates mix completely [19]. In a mixed layer new sites for the coadsorption layer are usually occupied. Adsorption of CO at low temperature on an oxygen atomic β_2-O_{ads} and β_1-O_{sub} states might produce a segregated layer and form islands of each species. Annealing of this adlayer up to ~160 K in TPR experiments leads to dispersing the islands and mixing the adsorbate layer at temperatures where reaction with CO is significant. The Pd–O bond is weakened in well-mixed O_{ads} + [$*O_{sub}$] + CO adlayer, indicating that the O_{ads}-[$*O_{sub}$] repulsive interaction proceeds throughout the metal surface rather than directly between the adsorbed atoms. On the other hand the effect of adsorbed oxygen (O_{ads} + [$*O_{sub}$]) on the CO adsorption rate is an important part of the low temperature CO oxidation reaction. Ladas *et al.* [20] have shown that the subsurface oxygen formation leads to the diminish of the CO residence time owing

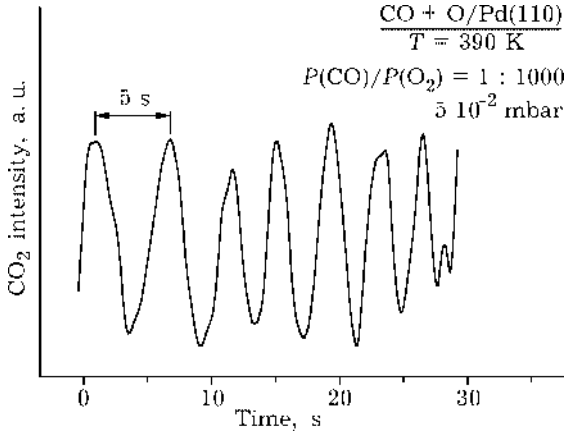

Fig. 5. Oscillatory behaviour of CO_2 production for the Pd(110) single crystal surface at constant control parameters.

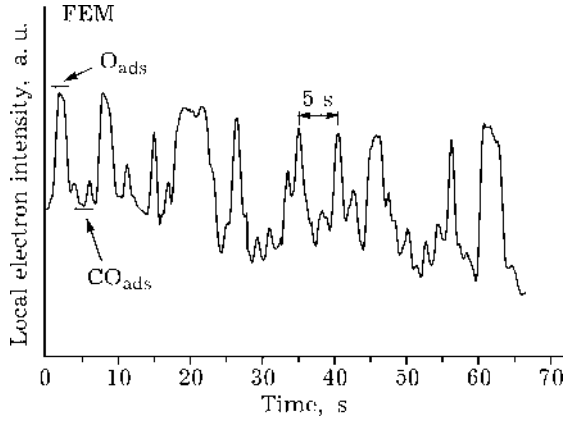

Fig. 6. The variation of the local emission current from the Pd $(100)_{step}$ plane as a function of time during the oscillatory behaviour of the CO + O_2 reaction on a Pd field emitter tip at constant control parameters under reaction conditions. T = 425 K, $P(O_2)$ = 2.6 10^{-3} mbar, P(CO) = 1.3 10^{-4} mbar. Low current levels reflect CO_{ads}-covered Pd(100) plane. $F \approx 0.4$ V/Å.

to a decrease of the CO adsorption energy and reduction of the CO sticking probability.

Hysteresis and oscillations

MB. Figure 4 illustrates the results of temperature dependence of the steady-state rate of CO oxidation over Pd(110) surface. At 300 K the reaction is limited by the activation of the surface reaction between CO_{ads} molecules and β_2-oxygen atoms as shown in Fig. 3, *a*. In the temperature interval 370–650 K the initial rate diminishes rapidly, presumably as a result of CO adsorption, which reduces the CO_{ads} coverage during the reaction. Figure 4 shows the bistability regions and represents the anticlockwise hysteresis behavior for the CO_2 formation in the temperature interval between 300 and 450 K. With temperature increasing the transfer from the θ_{CO} layer into the O_{ads} layer is delayed, with temperature decreasing it is the reverse reaction. The local single oscillations of the CO_2 rate at 372 and 382 K have appeared.

Figure 5 provides example of typical series of oscillations in the production of CO_2 when the Pd(110) single crystal surface is exposed at 390 K to a gas mixture of $P(O_2) = 5\ 10^{-2}$ mbar and P(CO) = 5 10^{-5} mbar. The oscillation amplitude ranges from the O_{ads} layer (high reactive state) to the O_{ads}/O_{sub} layer (low reactive state) with a periodicity of 5 s.

FEM. Figure 6 represents series of oscillations (FEM) when the Pd-tip with [110]-orientation is exposed at 425 K to a CO + O_2 reac-

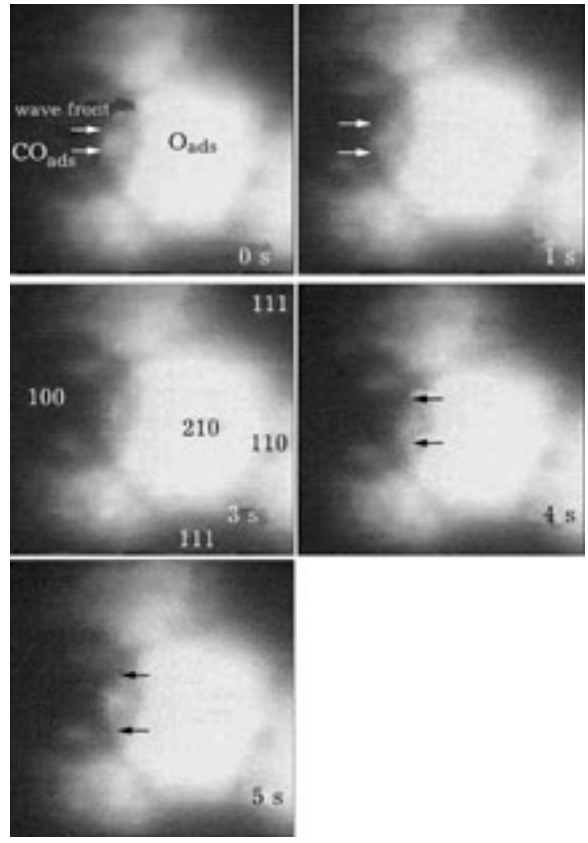

Fig. 7. Magnified view of a sequence of FEM images over (110)-oriented Pd-tip obtained during the CO + O_2 oscillating cycle at T = 425 K, $P(O_2)$ = 2.6 10^{-3} mbar, P(CO) = 1.3 10^{-4} mbar. At τ = 0–3 s formation of a large CO_{ads}-island (dark area over Pd(100) plane) and the (210) plane temporarily covered by oxygen O_{ads} layer appear bright. Moving reaction front during regular oscillation, starting from (100) towards (210) plane. At 3 s the CO_{ads} layer forms a final island size. After 4.0 s a reverse reaction front starts from (210) towards (100) plane.

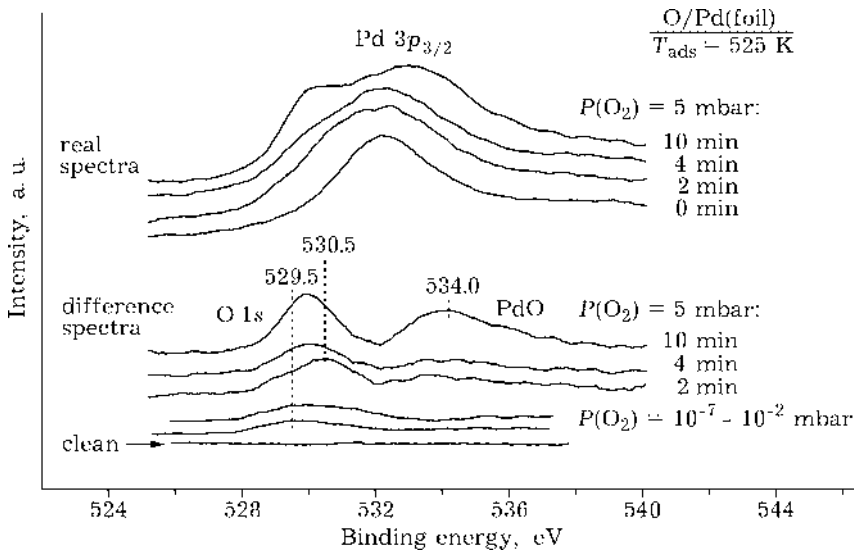

Fig. 8. XPS spectra for the clean, oxygen-covered and oxide growth Pd $3p_{3/2}$ at 45° take-off angle.

tion mixture. The oscillation amplitude from the CO_{ads} layer (low current) to the O_{ads} layer (high current) has a periodicity of 5 s. A difference of work functions between CO_{ads} and O_{ads} of ~0.6 eV is connected with a change in the electron current. The study of the Pd-tip surface has shown that the CO oxidation reaction is characterized by a sharp boundary between the two spatially separated adlayers (CO_{ads} and O_{ads}) over the $Pd\{100\}_{step}$ surfaces forming under oscillating conditions: 370 K < T < 450 K, $P(CO) + P(O_2)$ (1 : 20) = 2.6 10^{-3} mbar. The sequence of images in Fig. 7 corresponds to the following steps: the CO_{ads}-covered areas are formed only on the {100} nanoplanes, whereas O_{ads}- covered areas are formed only on the {110}, {310} and {210} nanoplanes. Chemical waves appear on an emitter surface and propagate in phase with self-sustained isothermal oscillations. The initiating role of a subsurface oxygen layer formation has been established for the generation of regular waves along the certain crystallographic directions on the Pd-tip surface: (i) O_{ads} wave follows the path in the direction (110) → (210) → (100); (ii) CO_{ads} wave moves in the opposite direction. The emission pattern brightness of local regions of the $Pd(100)_{step}$ surface was accompanied by a fluctuations of electron current. A difference of work function (ΔΦ) between CO_{ads} and O_{ads} over Pd surfaces is connected with a change in the emission current, as described by the Fowler − Nordheim equation:

$$I = AV^2 \exp(-B\Phi^{3/2} / V)$$

where I is the current measured at the fluorescent screen, V is the applied voltage at the tip, A and B are constants and Φ is the work function. From this equation a sensitive dependence of I on ΔΦ is expected. This large change in ΔΦ gives an excellent tool for observing the transition in the adsorbed layers: the CO adsorption layer with low emission current, current increases for oxygen adsorption. Using a conventional video technique to monitor the FEM brightness variation, local time oscillations of the emission current were extracted from digitized video images [21].

XPS. Figure 8 shows a set of Pd $3p_{3/2}$ XPS spectra for the Pd foil surface before and after oxygen exposure at 525 K. The difference spectra clearly show O 1*s* binding energy of 529.5 eV at surface coverage for atomic oxygen state ($P(O_2) = 10^{-7}$–10^{-2} Torr), which shifts to 530.5 eV after oxygen exposures for 2, 4 and 10 min at 5 mbar, showing the oxide growth. According to the XPS data, the state of palladium surface under the reaction oscillating conditions (370 < T < 450 K, $P(CO) + P(O_2)$ (1 : 20) = 2.3 10^{-3} mbar) is not sufficient for bulk oxide formation.

Reaction mechanism. The knowledge of the mechanism steps is necessary to gain a better insight into the oscillating phenomena. The oscillating catalytic CO oxidation proceeds via a Langmuir − Hinshelwood mechanism:

1. $CO_{gas} + * \leftrightarrow CO_{ads}$

2. $O_{2\ gas} + 2* \rightarrow 2O_{ads}$

3. $CO_{ads} + O_{ads} \rightarrow CO_{2\ gas} + 2*$

where two adjacent empty sites (*) are required for the dissociative adsorption of $O_{2\ gas}$. It is well known that under reaction conditions CO_{ads} islands are formed as well as O_{ads}, whereas CO_2 desorbs immediately.

The catalytic CO oxidation over palladium surfaces exhibits the temporal oscillations in certain range of reaction parameters: T, P_i. A feedback mechanism of these oscillations is associated with the changes in the sticking probability of oxygen (S_0) induced by depletion of subsurface oxygen (Pd(110): $O_{ads} \leftrightarrow O_{sub}$). The oxide model assumes that the O_{sub} layer blocks the oxygen adsorption simultaneously with the growth of CO_{ads} layer and the surface reaction is poisoned (low rate of CO_2 formation). The slow CO_{ads} reaction with O_{sub} removes the subsurface oxygen and O_2 adsorption is again possible (high rate of CO_2 formation). Then, the subsurface oxygen layer is formed and the cycle is restored. Probably, the subsurface oxygen could produce a significant change of CO adsorption energies, decreasing the heat of adsorption in according with [20].

Based on our TDS, TPR, XPS, MB, FEM data regarding to CO oxidation over Pd surfaces, some elementary steps have been added to LH scheme (scheme 1).

By this reaction scheme the model evolution was simulated with the standard Monte Carlo algorithm, that has been explored in our previous modeling of oscillatory behaviour of catalytic reactions due to the influence of the "subsurface" oxygen [22].

CONCLUSIONS

The palladium surface is catalytically active in CO + O_2 reaction due to the ability to dissociate O_2 molecules. At present, the O_{ads} diffusion process may be proposed for the formation of subsurface oxygen layer O_{sub}, which is an important intermediate species in CO + O_2 reaction over Pd surfaces. O_{ads} is highly active as compared to O_{sub} species due to the rapid attachment of the carbon monoxide molecules, CO_{ads}, producing CO_2. As a result of this oxidized surface the oscillations over the Pd(110) single crystal surface and the $Pd(100)_{step}$ nanoplanes can be obtained with fast repetition periods.

The specificity of the kinetics of CO + O_2 reaction has been observed over Pd tip: (i) the maximum initial rate has been observed on the Pd(110); (ii) two spatially separated adlayers are formed on the tip surface. The oxygen layer forms only on the {110}, {320} and {210} planes, whereas CO_{ads} layer or empty sites forms on the {100} and $\{100\}_{step}$ planes. Chemical waves are O_{ads} and CO_{ads} layers, interacting by a sequence of reaction steps with the reversible-oxygen sites transition of $O_{ads} \leftrightarrow O_{sub}$, which involves the feedback step $O_{sub} \rightarrow O_{ads}$ during oscillations.

CO oxidation over Pd surface (model with subsurface oxygen)

Atomic oxygen route (LH)	*Subsurface oxygen route (added)*
$O_{2\ gas} + 2* \rightarrow 2\ O_{ads}$	$O_{ads} + *_v \rightarrow [*O_{sub}]$
$CO_{gas} + * \leftrightarrow CO_{ads}$	$CO_{ads} + [*O_{sub}] \rightarrow CO_{2gas} + 2* + *_v$
$CO_{ads} + O_{ads} \rightarrow CO_{2\ gas} + 2*$	$CO_{gas} + [*O_{sub}] \leftrightarrow [CO_{ads}\ O_{sub}]$
	$[CO_{ads}\ O_{sub}] \rightarrow CO_{2gas} + *\ + *_v$<<cork-screw>> reaction

CO heat of adsorption: $q\ (CO_{ads}/[*O_{sub}]) < q\ (CO_{ads}/*)$

CO diffusion: $CO_{ads} + * \rightarrow * + CO_{ads} < [CO_{ads}\ O_{sub}] + [*O_{sub}] \rightarrow [*O_{sub}] + [CO_{ads}\ O_{sub}]$

Scheme 1.

In summary it may be said that the character of the CO + O_2 oscillating reaction on Pd differs remarkably from that of Pt: (i) subsurface oxygen mechanism (Pd) and phase transition mechanism hex ↔ 1×1 on Pt; (ii) oxygen front travelling in the reverse direction: on Pd starts from (110) to (100); on Pt starts from (100) to (110).

The principal result of this work lies in the following: the appearance of regular waves under the reaction rate oscillations is an amazing example of a self-organization of catalytic reaction when the size of active catalyst is some hundreds Angströms at average. It becomes possible to study the catalysis on an atomic level which is necessary for understanding of the mechanism of the action of the high-dispersion supported metal catalysts having the metal microcrystallites 100–300 Å in size as an active part of the catalyst. This result opens new fields for the development of theoretical concepts of heterogeneous catalysis.

Acknowledgements

This work is supported in part by RFBR Grant No. 02–03–32568 and INTAS Grant No. 99–01882.

REFERENCES

1 M. M. Slin'ko, N. I. Jaeger, Oscillating Heterogeneous Catalytic Systems. Surface Science and Catalysis, vol. 86, Elsevier, Amsterdam, 1994.
2 B. E. Nieuwenhuys, *Adv. Catal.*, 44 (2000) 259.
3 R. Imbihl, *Progr. Surf. Sci.*, 44 (1993) 185.
4 V. Gorodetskii, J. Lauterbach, W. Drachsel *et al.*, *Nature*, 370 (1994) 276.
5 M. F. H. van Tol, A. Gielbert, B. E. Nieuwenhuys, *Catal. Lett.*, 16 (1992) 297.
6 V. V. Gorodetskii, W. Drachsel, *Appl. Catalysis A: Gen.*, 4727 (1999) 1.
7 V. Gorodetskii, W. Drachsel, M. Ehsasi, J. H. Block, *J. Chem. Phys.*, 100 (1994) 6915.
8 G. Ertl, *Adv. Catal.*, 37 (1990) 213.
9 G. Veser, R. Imbihl, *J. Chem. Phys.*, 96 (1992) 7155.
10 P. D. Cobden, B. E. Nieuwenhuys, V. V. Gorodetskii, *Appl. Catal. A: Gen.*, 188 (1999) 69.
11 Yu. Suchorski, R. Imbihl, V. K. Medvedev, *Surf. Sci.*, 401 (1998) 392.
12 V. V. Gorodetskii, A. V. Matveev, P. D. Cobden, B. E. Nieuwenhuys, *J. Molec. Catal. A: Chem.*, 158 (2000) 155.
13 C. S. Gopinath, F. Zaera, *J. Catal.*, 186 (1999) 387.
14 V. A. Bondzie, P. Kleban, D. J. Dwyer, *Surf. Sci.*, 347 (1996) 319.
15 V. V. Gorodetskii, B. E. Nieuwenhuys, W. M. H. Sachtler, G. K. Boreskov, *Ibid.*, 108 (1981) 225.
16 W. A. Brown, R. Kose and D.A. King, *Chem. Rev.*, 98 (1998) 797.
17 M. Ehsasi, C. Seidel, H. Ruppender *et al.*, *Surf. Sci.*, 210 (1989) L198.
18 J.-W. He, P. R. Norton, *Ibid.*, 204 (1988) 26.
19 T. Engel, G. Ertl, *Adv. Catal.*, 28 (1979) 1.
20 S. Ladas, R. Imbihl, G. Ertl, *Surf. Sci.*, 280 (1993) 14.
21 M. C. Reckzügel, V. Gorodetskii, J. H. Block, *Appl. Surf. Sci.*, 49/95 (1996) 194.
22 E. I. Latkin, V. I. Elokhin, A. V. Matveev, V. V. Gorodetskii, *J. Molec. Catal. A: Chem.*, 158 (2000) 161.